COBEM 2021 26th International Congress of Mechanical Engineering
November 22-26, 2021, Virtual Congress, Brazil

COB-2021-1962
DIRECT HEATING OF SUPERCRITICAL CARBON DIOXIDE IN LINEAR FRESNEL COLLECTORS ANALYSIS

Ricardo Hofer Begrow
Júlio César Passos
Federal University of Santa Catarina – UFSC
Laboratory of Energy Conversion Engineering and Energy Technology – LEPTEN
88040-900, Florianópolis, SC, Brazil
r.begrow@gmail.com, julio.passos@lepten.ufsc.br

Abstract. *Recent advances in Fresnel technology have made it possible to reach temperatures above 500 °C, enabling the use of a sCO_2-based cycle. Both technologies are under development and have great potential for increasing efficiency and reducing costs. The present work aims the analysis of supercritical carbon dioxide (sCO_2) direct heating in linear Fresnel collectors for recompression Brayton cycle applications. The direct heating has the advantage of not using intermediate heat exchangers between the solar field and the power block, providing an efficiency increase and cost reduction. In addition, it eliminates the need for heating the molten salt circuit by electrical resistances during shutdowns. Thermal energy storage can still be used by dividing the solar field between CO_2 and molten salts, still partially presenting the listed benefits. The use of one or more absorber tubes were evaluated for direct heating, considering the pressure loss, heat loss and estimated cost. For reaching significant values, the pressure loss proved to be decisive in the choice of the receiver. SA-213 tubes with external machining were considered, with a wall thicknesses that support a maximum allowable working pressure (MAWP) above 20 MPa, according to the maximum allowable stresses of ASME Code Sections II and VIII. In several construction aspects, mainly in relation to evacuation, a single absorber tube with a glass tube enclosure, similar to that used in parabolic trough collector, proved to be preferable Considering thermal stress, the operation of an evacuated receiver with a flat glass cover can present significant challenges. In addition, evacuated tubes are commercially available and have high thermal efficiency, considering the selective surfaces available on the market, with an emissivity of up to 9.5% and an absorptivity greater than 94%. High pressures in the absorber requires some modifications to the available commercial evacuated tubes. Due to the corrosive characteristic of wet CO_2 and the high operating temperature, the use of a stabilized stainless steel, such as AISI 321, may be the best option. In addition, greater wall thickness is required. As the standard tubes of greater thickness have the same outside diameter as those of less thickness, there is no need for modifications to the glass enclosure, indicating the possibility of an easy adaptation of the industry.*

Keywords: *Supercritical carbon dioxide, direct heating, concentrated solar power, Fresnel, absorber design.*

1. INTRODUCTION

The recompression Brayton cycle has been promising in terms of thermal efficiency and cost reduction, having the potential to replace the steam Rankine cycles in power generation plants (White, 2016). At the same time, with the great demand for cheap and renewable energy sources, the Fresnel technology made significant advances. Linear Fresnel collectors (LFC) are simpler, cheaper and more durable (STELA, 2019) compared to other solar concentration systems. The absence of moving parts in the absorber reduces sealing costs and facilitates the use of direct heating of the working fluid, even high-pressure gases. This eliminates the need to use a heat transfer fluid and increases plant efficiency (Duffie and Beckmann, 2013). With evacuated receivers and secondary reflectors, it is possible to reach temperatures of up to 550°C, as proved in 2009 in a 1.4 MW power plant in Spain (HELIOCSP, 2011; Morin *et al*., 2014), making application possible in a supercritical CO_2 Brayton cycle. This work aims to analyze the main parameters of the receiver with sCO_2 direct heating in a LFC, as well as the heat transfer, the pressure loss and their relations with the collector dimensions.

1.1 Power cycle and collector performance

The performance of the supercritical CO_2 Brayton cycle and of the LFC were evaluated in relation to various parameters, considering various cycle configurations, in stationary condition and in design condition. Figure 1 shows the estimated collector efficiency and the combined efficiency of the collector and power cycle in relation to the turbine inlet temperature (TIT), for a direct normal incidence of 1000 W/m^2. It is observed that the combined efficiency peak of the collector and the power cycle occurs at approximately 550 °C for cycles with recompression (RC). For a pressure of 20

MPa, the advantage of using reheat (RH) and intermediate cooling (IC) is reduced as the TIT increases, achieving similar combined efficiency values at a temperature of 550 °C.

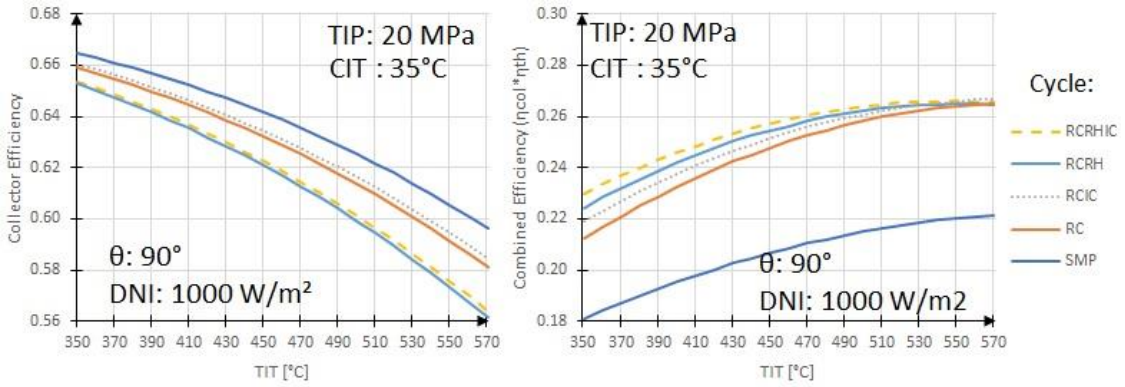

Figure 1. Collector efficiency and the combined efficiency of the collector and the power cycle.

1.2 The linear Fresnel collector and the sCO_2 direct heating

Direct heating of supercritical CO_2 in a high-concentration linear Fresnel collector has the advantage of not using intermediate heat exchangers between the solar field and the power block, providing an efficiency increase and cost reduction. Furthermore, the need for heating the molten salt in the plant by electrical resistances when it is inoperative is eliminated. For the use of thermal energy storage (TES), the solar field can be divided into a portion with CO_2, with solar multiple of 1, and the remainder using molten salts, still partially presenting the benefits listed, as shown in the schematic diagram in Figure 2, for a cycle with recompression and backup.

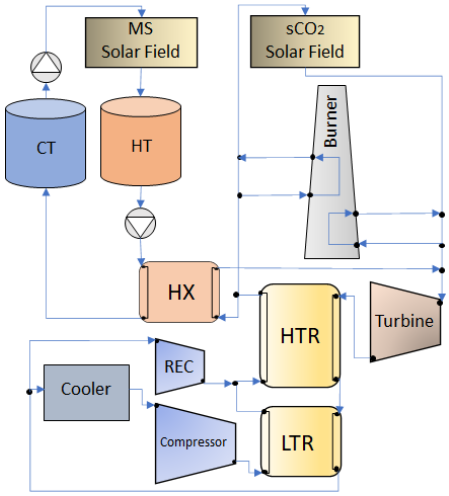

Figure 2. Schematic diagram of the power plant with direct heating, TES and backup.

In the case of using sCO_2 direct heating, the collector must withstand a pressure of approximately 20 MPa. It may be economically unfeasible to store CO_2 at this pressure, thus being subject to variations in solar incidence. These characteristics suggest the use of an intermediate fluid with TES and/or a backup system with fuels. Two types of receivers for sCO_2 direct heating were analyzed, shown in Figure 3. Tubes with glass envelope, similar to those used in parabolic-trough collector (PTC), are presented as an excellent option for use in a LFC. With evacuation, secondary mirrors and modern selective paints it is possible to reach high thermal efficiency even at high temperatures. Another simpler alternative is the use of several absorber tubes with selective paint, secondary plane reflectors and a flat glass cover (Figure 3.b). Lower thermal efficiency than single tube can be offset by a significant cost reduction. One of the disadvantages is the uneven heating of each absorber tube. However, the main challenge of this model may be to maintain an effective evacuation.

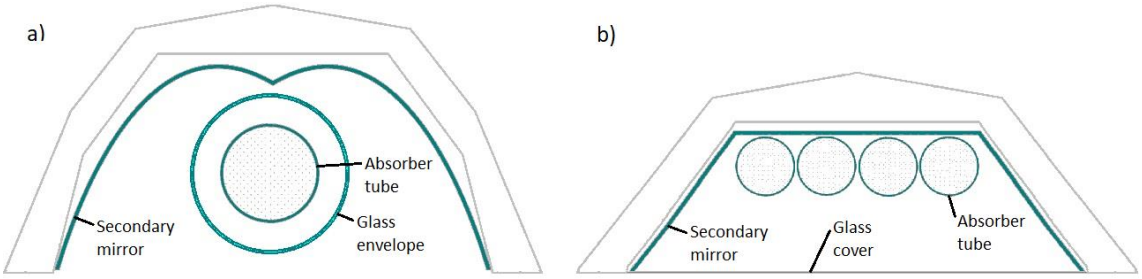

Figure 3. Evacuated receivers with secondary reflectors for linear Fresnel collectors.

1.3 Heat transfer in supercritical flow

The determination of heat transfer condition is necessary for modeling the main components of the cycle. In collectors, the convection heat transfer coefficient of the supercritical fluid represents the most important and limiting part of the total thermal conductivity. As the analysis of turbulent flow conditions is complex, its determination requires the use of empirical correlations that generally offer satisfactory precision within their recommended ranges. Errors can be reduced to less than 10% using more complex correlations (Incropera *et al*., 2007). For internal flow and high Reynolds number, the Gnielinski correlation (1987), shown in Eq. (1), can be used with high precision (Incropera *et al*., 2007), including the transition region for turbulent flow. The boundary of conditions where the correlation is valid is enclosed in square brackets.

$$Nu_D = \frac{(f/8)(Re_D - 1000)Pr}{1 + 12.7(f/8)^{1/2}(Pr^{2/3} - 1)} \quad ; \quad \begin{bmatrix} 0.5 \leq Pr \leq 2000 \\ 3000 \leq Re_D \leq 5\,.\,10^6 \end{bmatrix} \tag{1}$$

Where *Nu* is the Nusselt number, *Re* is the Reynolds number, *Pr* is the Prandtl number and *f* is the Darcy friction factor. Dimensional numbers are shown in Eq. (2).

$$Re_D = \frac{4\dot{m}}{\pi D_h \mu} \quad ; \quad Pr = \frac{c_p \mu}{k} \quad ; \quad Nu_D = \frac{hD_h}{k} \tag{2}$$

Where $\dot{m}$ is the mass flow rate, μ is the dynamic viscosity, D is the diameter, c_p is the specific heat at constant pressure, h is the convection heat transfer coefficient, and k is the thermal conductivity. For non-circular sections, the hydraulic diameter D_h is used. The friction factor f can be obtained from the Moody diagram or from correlations.

Vijayan *et al*. (2019) indicates that the heat transfer coefficients of supercritical fluids are close to those obtained by the Dittus-Boelter equation, except when very close to the critical point. More recent and specific correlations for supercritical fluids, such as the one by Mokry *et al*. (2011), use as a basis the Dittus-Boelter equation with some modifications, Eq. (3), where the Nusselt number (*Nu*) is defined as a function of the mean properties of the fluid in the volume, except for the specific mass of the fluid (ρ) in contact with the wall.

$$Nu_b = 0.0061\, Re_b^{0.9} \overline{Pr}_b^{0.68} \left(\frac{\rho_w}{\rho_b}\right)^{0.56} \tag{3}$$

The subscript *w* refers to the property of the fluid in contact with the tube wall and the subscript *b* refers to the average property of the fluid (bulk). The use of this equation is suggested by Pioro *et al*. (2016) as the most accurate in relation to several experimental results for supercritical water. However, when it comes specifically to sCO_2, Pioro *et al*. (2016) developed Eq. (4), based on updated thermodynamic properties from Lemmon *et al*. (2010). This equation was modeled to include the pseudocritical region. The mean Prandtl number in this equation is defined in relation to the mean specific heat. The dimensionless numbers of the fluid in contact with the wall are obtained using the properties of the fluid in contact with the wall.

$$Nu_w = 0.0038\, Re_w^{0.96} \overline{Pr}_w^{-0.14} \left(\frac{\rho_w}{\rho_b}\right)^{0.84} \left(\frac{k_w}{k_b}\right)^{-0.75} \left(\frac{\mu_w}{\mu_b}\right)^{-0.22} \tag{4}$$

1.4 Pressure loss in supercritical flow

Pressure loss, as well as heat loss, plays a fundamental role in the correct modeling of the cycle. In some components, such as heat exchangers and receivers, it can have a significantly high value. The pressure loss in the supercritical CO_2

flow was estimated by the Darcy friction factor using the Niazkar solution (2019), which is based on the modified Serghides equation (1984). These equations, in turn, are the direct solution of the Colebrook–White equation, Eq. (5), which is expressed in relation to the Reynolds number and the relative roughness (ε).

$$\frac{1}{\sqrt{f}} = -2\,log\left(\frac{\varepsilon}{3.7D_h} + \frac{2.51}{Re\sqrt{f}}\right) \qquad ; \qquad [Re > 4000] \tag{5}$$

A direct solution of the Colebrook–White equation is obtained in an approximation by the Steffensen method (Niazkar, 2019), resulting the Niazkar equation, Eq. (6).

$$\frac{1}{\sqrt{f}} = A - \frac{(B-A)^2}{C - 2B - A} \tag{6}$$

Where:

$$A = -2\log\left(\frac{\frac{\varepsilon}{D}}{3.7} + \frac{4.5547}{Re^{0.8784}}\right) \quad ; \quad B = -2\log\left(\frac{\frac{\varepsilon}{D}}{3.7} + \frac{2.51A}{Re}\right) \quad ; \quad C = -2\log\left(\frac{\varepsilon/D}{3.7} + \frac{2.51B}{Re}\right) \tag{7}$$

With the Darcy friction factor, the pressure loss (Δp) is obtained by the Darcy–Weisbach equation, Eq (7). Where L is the considered section of the tube and v is the flow velocity.

$$\frac{\Delta p}{L} = f\,\frac{\rho}{2}\frac{v^2}{D_h} \tag{8}$$

2. ABSORBERS ANALYSIS AND SPECIFICATION FOR DIRECT HEATING

The dimensioning of the absorber tubes was done in accordance with ASME code, Section VIII, Division 1, for pressure vessels, for an internal pressure of 200 bar and a nominal diameter of up to three inches. For pressures greater than 200 bar, Division 2 of this same code must be used, with stricter and more precise rules for stress determinations (ASME, 2019). Also, according to the maximum allowable stresses of Section II, considering a temperature of up to 550 °C in the collector, calculations shown that tubes schedule 80 and 160 are required.

2.1 Materials

The materials considered for the application were those recommended for heat exchanger tubes (Telles, 1996), such as carbon steel (ASTM SA-179), high temperature carbon steel (ASTM SA-106 B), molybdenum steel (ASTM SA-209) and chromium-molybdenum steel (SA-213 series). The use of austenitic stainless steel, such as AISI 304 and AISI 316, was also considered, due to the corrosive characteristic of carbon dioxide when contaminated with moisture (Rodrigues *et al*., 2014). The steels listed have a satisfactory strength limit at room temperature, however, there is a decrease in the maximum allowable stress as the temperature increases (ASME, 2010), resulting in significant differences in the required thickness.

2.2 Corrosion and temperature influence

Tests performed by Rodrigues *et al*. (2014) on carbon steel indicate that, for pressures above the critical pressure of wet CO_2, the corrosion rate increases with pressure. For a pressure of 10 MPa, the corrosion rate is 8.6 μm/a and reaches a value of 0.063 mm/a for a pressure of 20 MPa. Thus, carbon steels can have considerable corrosion due to the contamination of sCO_2 with humidity. Furthermore, carbon steels present the greatest loss of strength with the increase in temperature of the steels considered, mainly due to time dependent deformations (creep), which begin to be observed from 370 °C onwards (Telles, 1996). With these characteristics, the use of carbon steel is not indicated, except for low temperatures and high humidity control.

Telles (1996) indicates that stainless steels should be used for corrosive environments and temperatures above 450 °C. Also, according to the author, steels with L termination, despite showing high resistance to intergranular corrosion, have reduced mechanical resistance for temperatures above 400 °C. Thus, for corrosive media above 450 °C, stabilized stainless steels, such as AISI 321, are more suitable. AISI 321 steel is stabilized against the formation of chromium carbide by the addition of titanium, while AISI 347 and 348 steels are stabilized by the addition of niobium and tantalum (NIDI, 1993). Due to the considerable cost of stainless steels, the use of alloy steels as a means of dehumidifying the working fluid may be more economical. Figure 4 shows the variation of the maximum allowable voltage adapted from the ASME

code, Section II, Part D (2010), for the considered steel pipes. It is observed that stainless steels have greater resistance at high temperatures compared to the others materials considered, resulting in smaller thicknesses and partially offsetting its high cost. However, stainless steels have a thermal conductivity of approximately 20 W/m.K, against approximately 40 W/m.K of the low-alloy steels (Brandes and Brook, 1998).

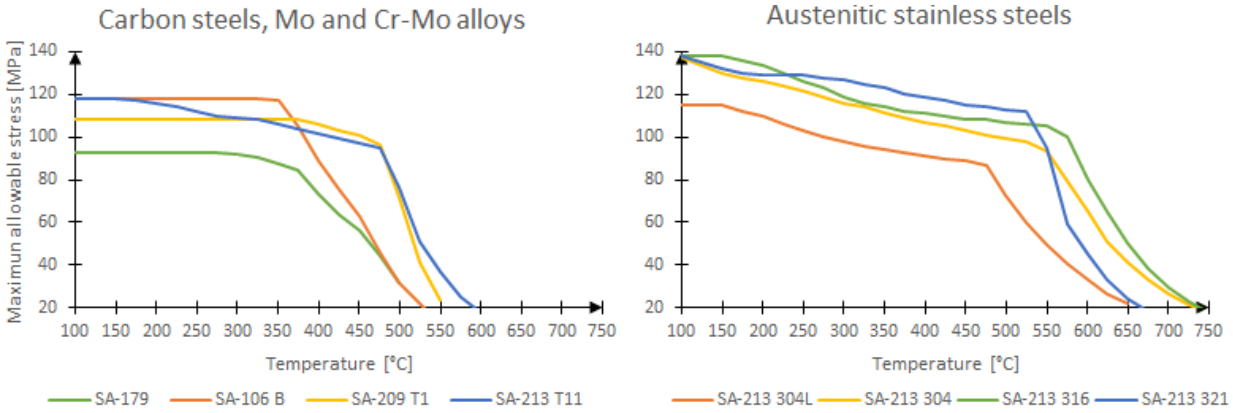

Figure 4. Maximum allowable stress according to ASME BPVC, Section II, Part D (2010).

2.3 Pressure loss and heat loss

The sCO_2 viscosity, as with most gases, is relatively low. In the operating ranges of the supercritical cycle, its value varies from approximately 20 to 35 μPa.s. (Lemmon *et al*., 2010). This enables high flow velocities, which cause a significant increase in turbulence and heat transfer coefficient. The flow velocity is generally limited by possible internal erosion of components and acceptable pressure loss (Shah and Sekulic, 2003).

The pressure loss in the sCO_2 flow was estimated using the Niazkar (2019) solution. Figure 5 shows the pressure drop as a function of temperature, velocity and mass flow in a 2.1/2 in. pipe. Figure 4.b) shows the usual operating region of an LFC with direct heating.

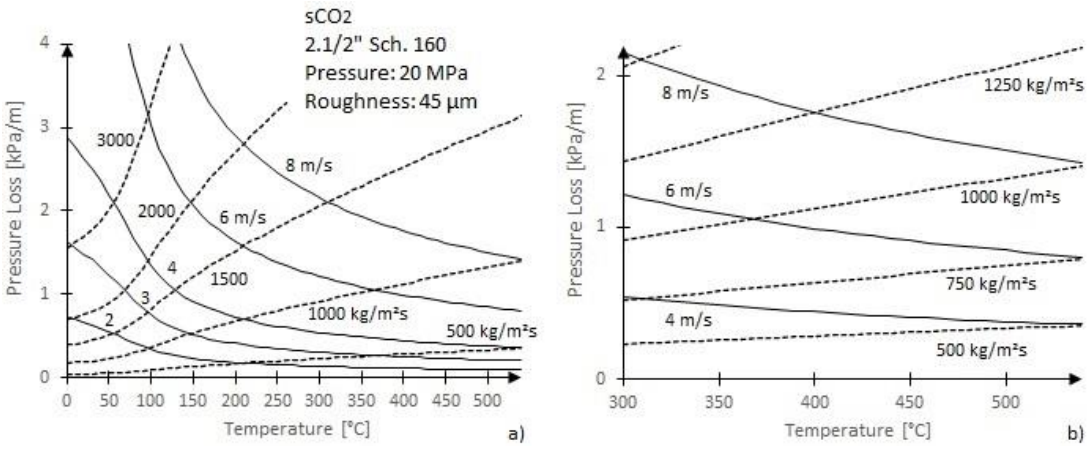

Figure 5. sCO_2 pressure loss in relation to temperature, velocity and mass flow in a 2.1/2 in. tube.

The use of one or more absorber tubes was evaluated for direct heating in receivers, considering pressure loss, heat loss and estimated cost. The pressure loss, for reaching significant values, proved to be decisive in the choice of absorber. Figure 6 shows the calculated pressure loss and mass flows in an admissible range for two Fresnel collectors, one 96 meters long and the other 50 meters long, for various diameters. Increasing the length of the collector significantly increases the internal mass flow, making it necessary to use larger diameters for a reasonable pressure loss.

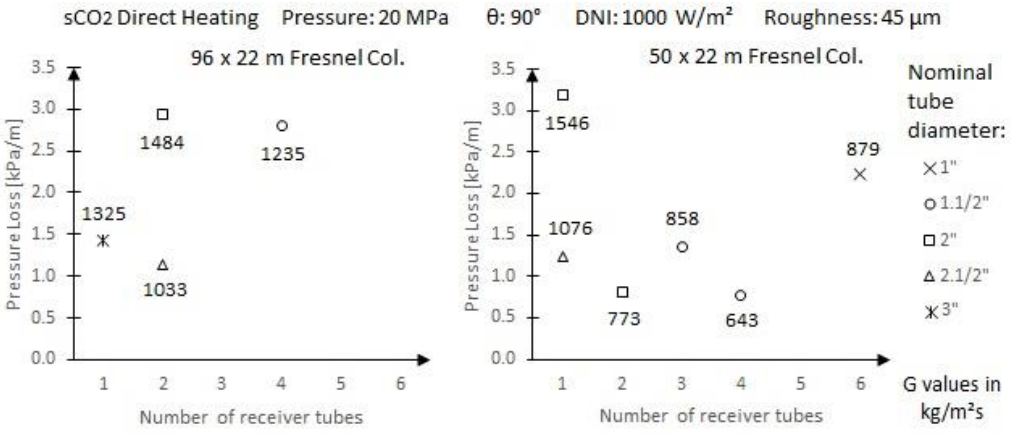

Figure 6. Pressure loss and mass flow in the absorbers for various diameters and number of tubes.

For a single absorber tube, a standard evacuated tube was considered, with a inner steel tube and a tubular glass envelope (Figure 2.a). For two or more tubes, steel tubes with selective painting in an evacuated receiver with a flat glass cover were considered (Figure 2.b). The average roughness was defined as 45 µm inside the tubes. In this case, the fluid enters the receiver at a temperature of approximately 370 °C, where it is heated to approximately 500 °C. The use of a single absorber tube (Figure 2.a) proved to be preferable in several constructive aspects, especially in relation to evacuation. Considering thermal stress, operating an evacuated receiver with a flat glass cover can present significant challenges. Also, evacuated tubes are commercially available and feature high thermal efficiency. Figure 7 shows the receiver estimated heat loss for different diameters in relation to the absorber surface temperature, considering a selective surface available on the market, with emissivity of up to 9.5% and absorptivity of 94%.

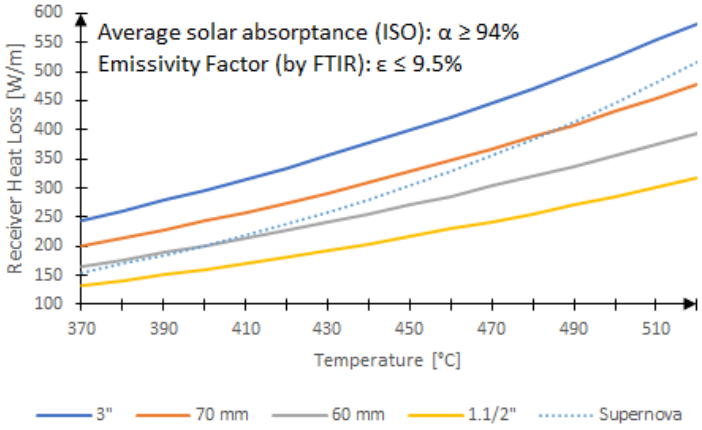

Figure 7. Receiver heat loss from for different diameters in relation to absorber surface temperature.

The average thermal efficiency of the collector with direct heating was estimated for a sCO_2 cycle operation, with a turbine inlet temperature of 500 °C, as shown in Table 1. Different diameters were considered, all with a pressure loss of 1 bar.

Table 1. Average thermal efficiency of the absorber in relation to diameter in sCO_2 direct heating cycle. TIT = 500 °C. DNI = 1000 W/m^2. Pressure loss = 1 bar.

Diameter	Average heat loss [W/m]	Average thermal efficiency [-]
3”	381	0.599
70 mm	310	0.602
60 mm	253	0.597
1.1/2"	202	0.594

The relation of pressure loss to total collector length and mass flow is shown in Figure 8, for a 22 meter wide and 11 meter wide collector. It can be seen that each collector length has a range of acceptable diameters. The mirror

configuration used was similar to the Solar Power Group SPG type 3 collector, for direct heating of CO_2 in a single absorber tube. It is observed that the total pressure loss increases approximately in a cubic function with increasing length of the collector and approximately in a quadratic function with increasing width. The pressure loss per unit of length, on the other hand, has a quadratic relation with both dimensions of the collector. This indicates that each absorber diameter only serves a mirrored area of specific dimensions.

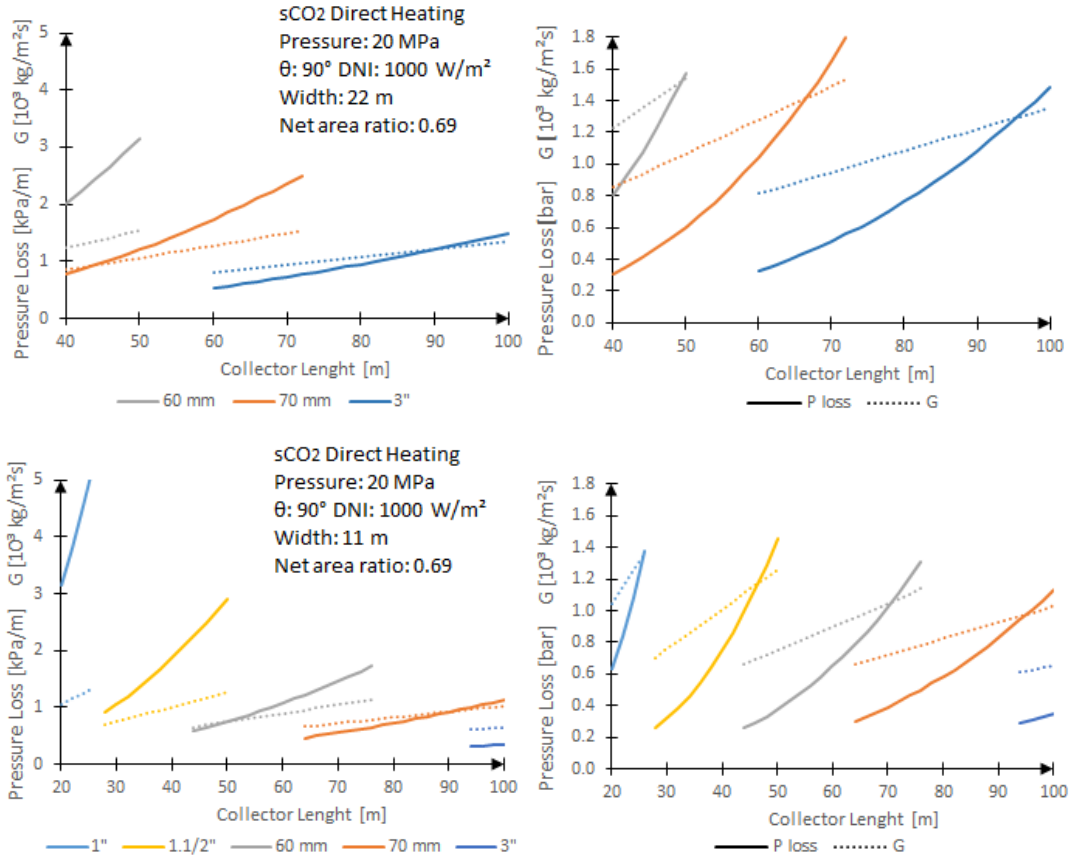

Figure 8. Pressure loss for a single absorber tube in relation to total length and mass flow.

2.4 Heat transfer coefficient and tube wall temperature

As well as the pressure loss, the heat transfer coefficient is dependent on the dimensions of the mirrored area of the collector, as this defines the mass flow and consequently the flow velocity. The same is true for the external temperature of the absorber tube. The heating of the fluid inside the tube causes an acceleration of the flow, which affects the coefficient of heat exchange by convection, as well the external temperature of the tube, the loss of energy by radiation and, consequently, the heating of the fluid itself. Thus, the modeling requires discretization of the absorber tube. Equation (9) shows the energy balance on the discretized surface in a timeless way, in relation to the heat absorbed by the tube ($q_{abs,T}$) and the heat absorbed by the fluid ($q_{abs,F}$), disconsidering conduction heat losses at the joints and convection losses in the evacuated environment.

$$q_{abs,T}(i) = q_{abs,F}(i) - q_{loss,T}(i) \tag{9}$$

Substituting the terms in the energy balance, we obtain Eq. (10). The exact solution for the external temperature of the absorber tube (T_T) in steady state requires solving a fourth power equation.

$$A_{col}(i).r_A.DNI.cos\theta.\eta_{opt}.\tau_{gl}.\alpha_T = \frac{T_T(i) - T_b(i)}{D_{T,in}\frac{\ln(D_{T,o}/D_{T,in})}{2k} + \frac{1}{h}} + \pi.D_{T,o}.L_T(i).\sigma.\varepsilon_T(T_T^4(i) - T_{amb}^4) \tag{10}$$

Where h is the heat transfer coefficient by convection inside the tubes, which also depends on the dimensions of the solar collector. $A_{col(i)}$ is the discretized area of the collector, r_A is the ratio between the mirrored area and the area of the collector, DNI is the solar direct normal incidence, θ is the solar incidence angle, η_{opt} is the optical efficiency of the

collector, τ_{gl} is the transmittance of the glass envelope, α_T is the absorptivity of the tube surface, ε_T is the emissivity of the tube surface, $L_T(i)$ is the discretized length of the tube, T_{amb} is the ambient temperature, T_b is the mean fluid temperature and σ is the Stefan–Boltzmann constant. The solution of Eq. (10) shows that the temperature difference between the outer surface of the absorber tube and the temperature of the fluid inside the tube varies with the dimensions of the mirror surface and the diameter of the absorber. However, the most significant variable is the tube wall thickness. As solving the equation can be complex for an analysis of all variables, an approximation was performed, where the tube surface temperature (T_T) is replaced by the fluid temperature (T_b) in the term referring to thermal loss by radiation ($q_{abs,F}$):

$$T_T^4(i) \approx T_b^4(i) \tag{11}$$

The solution of Eq. (10) with the simplification of Eq. (11) results in a maximum error of 0.7% in the temperature difference between the fluid and the tube's external temperature. This value represents a maximum absolute error of 0.1 °C. With a new iteration, substituting again the approximate wall temperature in Eq. (10), an absolute error 0.0004 °C is obtained. In the extension of the collector, the heat transfer coefficient increases linearly and the temperature difference diminishes infinitely in the direction of the flow, being approximately constant, as shown in Figure 9, for several collectors with pressure loss of 1 bar.

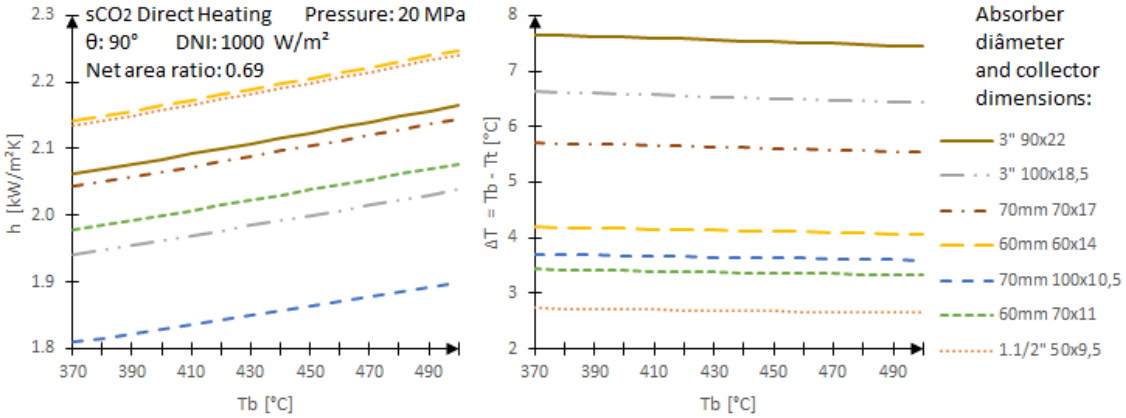

Figure 9. Heat transfer coefficient and temperature difference between the surface and the fluid in the absorber.

In the cases studied, for an incidence of 1000 W/m^2, the temperature difference does not exceed 10 °C and the average heat transfer coefficient is approximately 2 kW/m^{2}K. In steady state, the temperature difference between the outer surface of the absorber tube and the fluid temperature inside the tube is approximately constant throughout. In this way, it is possible to use the average temperature difference without significant errors. Figure 10 shows the temperature difference between the fluid and the surface of the absorber and the heat transfer coefficient for different tube diameters, in relation to the length of the collector, for a collector 11 meters wide and another 22 meters wide. It is observed that the temperature difference increases with the increase of the collector width and the tube diameter.

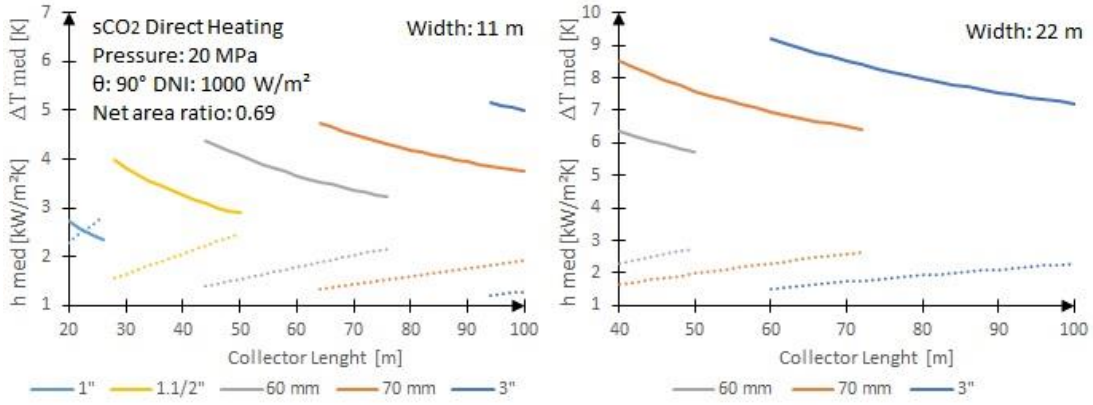

Figure 10. Average heat transfer coefficient and the average temperature difference between the absorbing surface and the fluid in relation to the total length of the collector.

3. EVACUATED TUBES ADEQUATION FOR DIRECT HEATING

The use of high pressures in the absorber requires some modifications to the usual evacuated absorber tubes, which basically boils down to changing the thickness of the inner steel tube. As the thicker standard tubes have the same outer diameter as the thinner ones, there is no need for modifications to the glass casing. Considering the maximum allowable stresses for stainless steels, Table 2 was prepared, which shows the maximum allowable working pressure for SA-213 pipes with external machining. For heating supercritical CO_2 up to 500 °C, stabilized stainless steels such as AISI 321 and 347 are most recommended. Low carbon stainless steels with the "L" termination are not suitable for this operating temperature. AISI 321 tubes with a diameter of 60 mm are the most cost-effective option for direct heating up to 220 bar. For pressures above 250 bar, AISI 321 Sch. 160 pipes stand out when machined to 70 mm. Both can be fitted with standard sized commercially used glass cases.

Table 2. Maximum allowable working pressures for machined seamless tubes SA-213 for sCO_2 direct heating.

Nominal diameter [in]	External diameter [mm]	Schedule	Original thickness [mm]	Internal diameter [mm]	Machined diameter [mm]	Material	PMTA (500 °C) [bar]	PMTA (550 °C) [bar]
3	88.9	80	7.62	73.66	88	AISI 321	197	165
						AISI 347	200	174
		160	11.13	66.64	85	AISI 316	253	248
						AISI 321	267	224
2.1/2	73	80	7.01	58.98	72	AISI 316	209	205
						AISI 321	220	184
						AISI 347	224	195
		160	9.53	53.94	70	AISI 316	270	265
						AISI 321	285	239
2	60.3	80	5.54	49.22	60	AISI 316	207	203
						AISI 321	219	183
1.1/2	48.3	80	5.08	38.14	48	AISI 316	239	235
						AISI 321	253	212

4. CONCLUSION

Various parameters were analyzed in relation to the supercritical carbon dioxide direct heating, in a high concentration linear Fresnel collector with an evacuated receiver, mainly in relation to the absorber, for applications in a Brayton cycle. Thermodynamic and constructive aspects of the absorber were evaluated, such as pressure loss, heat loss, heat transfer coefficient, material selection, corrosion, dimensioning and its suitability in relation to commercial pipes. These aspects were evaluated at the combined thermal efficiency peak temperature of an LFC and a sCO_2 recompression Brayton cycle, which is approximately 500 °C for a perpendicular solar incidence of 1000 W/m^2. Direct heating of supercritical CO_2 appears to be feasible at pressures of 20 MPa or more, using evacuated tubes in the collectors. With the increase in the internal thickness of the absorber tube, it can withstand high pressures without the need for any external alterations, indicating an easy adaptation of the industry. Thus, a hybrid system with direct heating of supercritical CO_2 and indirect heating with molten salts was proposed, which combines the characteristics of both systems and maintains the advantages of direct heating and thermal storage. The use of CFL for power generation technology under development, as is the use of supercritical CO_2 in power cycles. Both have great potential to reduce costs and increase efficiency. Recent advances in Fresnel technology have provided the synergy needed to integrate these two technologies, which could significantly change the way solar energy is used.

5. ACKNOWLEDGEMENTS

This work was realized with financial support of PETROBRAS (ANEEL: PD-00553-0042/2016), through the Teaching and Engineering Foundation of Santa Catarina (FEESC).

6. REFERENCES

ASME, 2010. *Boiler and Pressure Vessel Code: Section II – Materials. Part D, Properties (Metric).* American Society of Mechanical Engineers.

ASME, 2019. *Boiler and Pressure Vessel Code: Section VIII – Rules for Construction of Pressure Vessels, Division 1*. American Society of Mechanical Engineers.

Brandes, E. A. and Brook, G. B., 1998. *Smithells Metals Reference Book*. Butterworth-Heinemann, 7th ed.

Duffie, J. A. and Beckmann, W. A., 2013. *Solar Engineering of Thermal Processes*. John Wiley & Sons, Inc., 4th ed.

Gnielinski, V., 1976. "New equations for heat and mass transfer in turbulent pipe and channel flow". *International Chemical Engineering*. Vol. 16.

HELIOCSP, 2011. "Novatec Solar's Fresnel collector generates superheated steam above 500°C". http://helioscsp.com/novatec-solars-fresnel-collector-generates-superheated-steam-above-500c/. Accessed in 12 Sep. 2019.

Incropera, F. P., Dewitt, D. P., Bergman, T. T. and Lavine, A. S., 2007. *Fundamentals of heat and mass transfer*. 6th ed. John Wiley & Sons.

Lemmon, E. W., Huber, M. L. and Mclinden, M. O., 2010. *NIST Standard Reference Database 23*: *Reference Fluid Thermodynamic and Transport Properties – REFPROP*. Version 9.0. National Institute of Standards and Technology, Standard Reference Data Program. Gaithersburg.

Mokry, S., Pioro, I., Farah, A., King, K., Gupta, S., Peiman, W. and Pavelkirillov, P., 2011. "Development of Supercritical Water Heat-Transfer Correlation for Vertical bare Tubes". *Nuclear Engineering and Design*. Vol. 241.

Morin, G., Karl, M., Mertins, M., and Selig, M., 2014. "Molten Salt as a Heat Transfer Fluid in a Linear Fresnel Collector – Commercial Application backed by Demonstration". *International Conference on Concentrating Solar Power and Chemical Energy Systems*.

Niazkar, M., 2019. "Revisiting the Estimation of Colebrook Friction Factor: A Comparison between Artificial Intelligence Models and C-W based Explicit Equations". *KSCE Journal of Civil Engineering*.

NIDI, 1993. *Design Guidelines for the Selection and Use of Stainless Steel*. n. 9014. Nickel Development Institute. Specialty Steel Industry of North America.

Pioro, I., Gupta, S. and Mokry, S., 2012. "Heat-Transfer Correlations for Supercritical-Water and Carbon Dioxide Flowing Upward in Vertical bare Tubes". *ASME 2012 Summer Heat Transfer Conference*. Rio Grande, Puerto Rico.

Rodrigues, T. R. S. A., Da Costa, E. M., Marcolino, J. B. and De Moraes, M. K., 2014. "Corrosion of carbon steel by CO_2: Influence of pressure on the corrosion rate (in Portuguese)". *21st CBECIMAT - Brazilian Congress of Engineering and Materials Science*. Cuiabá, MT, Brazil,

Serghides, T. K., 1984. "Estimate friction factor accurately". *Chemical Engineering Journal*. n. 91.

Shah, R. K. and Sekulic, D. P., 2003. *Fundamentals of heat exchanger design*. John Wiley & Sons.

STELA, 2019. *Linear Fresnel Reflectors*. World Solar Thermal Electricity Association. http://www.stelaworld.org/linear-fresnel-reflectors/. Accessed in 14 oct. 2019.

Telles, P. C. S., 1996. *Pressure vessels* (in Portuguese). LTC, 2nd ed. Rio de Janeiro, Brazil.

Vijayan, P. K., Nayak, A. K. and Kumar, N., 2019. *Single-phase, Two-phase and Supercritical Natural Circulation Systems*. Woodhead Publishing. 1st ed.

White, C., 2016. "Analysis of Brayton Cycles Utilizing Supercritical Carbon Dioxide", DOE/NETL-4001/070114, In Preparation. Rev. 1, NETL.

7. RESPONSIBILITY NOTICE

The authors are the only responsible for the printed material included in this paper.